Journal of
Materials Chemistry C

Accepted Manuscript

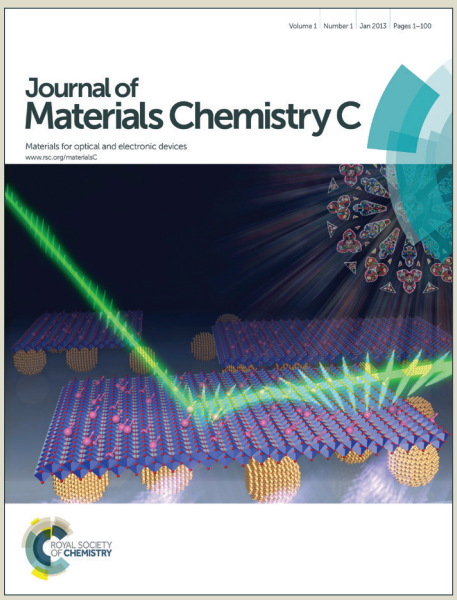

ROYAL SOCIETY OF CHEMISTRY

www.rsc.org/materialsC

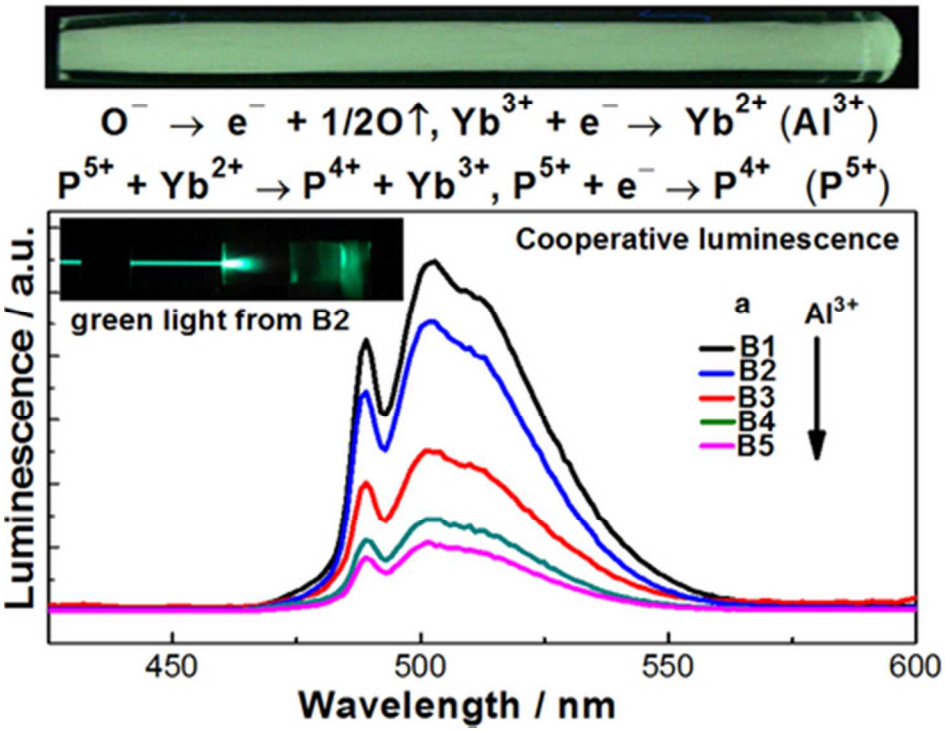

The graph for table of contents entry
39x30mm (300 x 300 DPI)

Cite this: DOI: 10.1039/c0xx00000x

www.rsc.org/xxxxxx

ARTICLE TYPE

Influences of the Al^{3+} and P^{5+} ions contents on the valence state and the dispersion effect of Yb^{3+} ions in silica glass

S. Wang,*[a,b] F. Lou,[a,b] C. Yu,[a] Q. Zhou,[a] M. Wang,[a] S. Feng,[a] D. Chen,[a] L. Hu,[a] W. Chen,[a] M. Guzik,[c] G. Boulon[d]

Received (in XXX, XXX) XthXXXXXXXXX 20XX, Accepted Xth XXXXXXXXX 20XX
DOI: 10.1039/b000000x

Three series of Yb^{3+}-doped silica glasses containing different amounts of Al_2O_3 and P_2O_5 were prepared successfully by using sol-gel method. Absorption, excitation and fluorescence spectra of Yb^{2+} ions in these silica glasses as well as the X-ray photoelectron spectroscopy (XPS) of Yb4d were measured and analysed systematically. It is found out that the addition of Al^{3+} or P^{5+} ions has a great influence on the redox state of ytterbium ions. With increasing Al^{3+} ions content in these silica glasses, more trivalent Yb^{3+} ions are reduced to divalent Yb^{2+}. On the contrary, the increase of P^{5+} ions content greatly promotes divalent Yb^{2+} ions to be oxidized into trivalent Yb^{3+}. The possible redox mechanisms have been explored and discussed in detail. The influences of Al^{3+} and P^{5+} ions contents on the near-infrared luminescence intensity of Yb^{3+} ions and cooperative luminescence of Yb^{3+} ions pairs were also discussed. Both the near-infrared luminescence intensity of Yb^{3+} ions and cooperative luminescence of Yb^{3+} ions pairs decrease gradually with increasing Al^{3+} and P^{5+} ions contents. The decrease of cooperative luminescence of Yb^{3+} ions pairs indicates good dispersion effect of Yb^{3+} ions by Al^{3+} and P^{5+} ions in Yb^{3+}-doped silica glass. The results are useful for optimization of fabrication process of the high quality Yb^{3+}-doped silica fiber by composition design of Yb-Al-P co-doped silica glass.

1. Introduction

In recent years, Yb^{3+}-doped silica fiber lasers have become a hot research area [1−6] because of the demand for high-power fibre lasers from Inertial Confinement Fusion (ICF) [7] and laser processing. High-power fiber sources that maintain a good output beam quality are often realized by using a Yb^{3+}-doped silica large-mode-area photonic crystal fiber (LMA PCF) (i.e., large core and low NA) to reduce optical intensity in the core whilst guiding single-mode or only a small number of mode at certain designed PCF structures [8−9].Therefore, Yb^{3+}-doped LMA PCF can be applied to high-power single-mode laser devices. Generally, high Yb^{3+} doping concentration is necessary to reach sufficient pump absorption even in a cladding pumped configuration. This reduces the fiber length and increases the threshold for undesirable nonlinear effects in the fiber [8]. In this regard, co-doping with Al^{3+} or P^{5+} ions in silica glass is the most effective way to increase Yb^{3+} solubility in silica glass and avoid clustering due to their good "dispersion effect" of ytterbium ions [10−13].

Induced optical loss, also called photodarkening (PD), is known to be a detrimental process limiting the performance of Yb^{3+}-doped silica fiber lasers in many applications [14−15]. Earlier studies have shown that the PD rate is correlated to the number density of Yb^{3+} ions in the excited state [16] and clustering of Yb^{3+} ions results in PD [15]. A reduction of PD was qualitatively described for fiber with enhanced Al^{3+} ions co-doping [17]. Moderate addition of P^{5+} ions has a better effect on suppressing PD in Yb^{3+} and Al^{3+} ions co-doped silica fiber [8, 18]. Meanwhile, the addition of P^{5+} ions together with Al^{3+} ions can reduce the refractive index of the fiber core [14]. Especially, when Al^{3+} and P^{5+} ions are co-doped in equimolar amounts, the refractive index of the doped-core glass approaches that of pure silica [8]. Although many studies have adopted Al^{3+} and P^{5+} ions co-doping to enhance Yb^{3+} ions doping levels in silica glass or fiber and suppressing PD, very few studies have discussed the effects of Al^{3+} and P^{5+} ion contents on the formation of Yb^{2+} and spectral properties of Yb^{2+} and Yb^{3+}ions in silica glass. Yb^{2+} ions can be easily formed and co-exist with Yb^{3+} ions when silica glass or fiber is prepared under reducing conditions. Furthermore, co-doping of Al^{3+} or P^{5+} ions in silica glass can affect the valence of ytterbium ions [19−20].Yb^{2+} ions have intense and broad absorption bands at the UV and visible regions, and the intensities of those absorption bands are more than ten times stronger than those of Yb^{3+}ions [21]. The tail of these absorption bands extends to near-infrared region (beyond Yb^{3+}ion absorption), which leads to a remarkable increase in fiber background loss [22]. Eventually, Yb^{2+} ions can directly impair the lasing level of Yb^{3+}ions, reduce the fluorescence lifetime and slope efficiency, and induce PD [22−23]. Recent research suggests that Yb^{2+} ions play an important role in PD process and a small number of Yb^{2+} ions can generate in PD process caused by charge transfer (CT) transition [24].

Early studies have described the reducing effects of Al^{3+} on Eu^{3+} and Sm^{3+} in aluminosilicate glass during sintering or heating in a H_2 gas atmosphere [25−26]. To the best of our knowledge, no reports on the influences of Al^{3+} and P^{5+} ions contents on redox states of ytterbium ions in silica glass are available. In this work, a sol-gel method combined with high temperature sintering was adopted to prepare Yb^{3+}-doped silica glass as fiber preform core [27]. Compared with traditional MCVD method, large-size glass

samples with broad composition region can be prepared by sol-gel method. Al_2O_3 and P_2O_5 can be easily and homogeneously doped into SiO_2 glass by this method. Three series of Yb^{3+}-doped silica glasses with different amounts of Al^{3+} and P^{5+} ions were prepared to investigate the effects of Al^{3+} and P^{5+} ions contents on redox of ytterbium ions. The influences of Al^{3+} and P^{5+} ions contents on the near-infrared luminescence intensity of Yb^{3+} ions and cooperative luminescence of Yb^{3+} ions pairs were also discussed to study the dispersion effect of Yb^{3+} ions by Al^{3+} and P^{5+} ions.

2. Sample preparation and characterization

Tetraethoxysilane (TEOS), C_2H_5OH, $AlCl_3$•$6H_2O$ (Aladdin, 99.99%), H_3PO_4 (Sigma-Aldrich, 99.999%) and $YbCl_3$•$6H_2O$ (SAFC, 99.998%) were used as precursors. Deionized water was added to sustain the hydrolysis reaction. The preparation process of Yb^{3+}-doped silica glass by sol-gel method has been described in detail in reference [27]. It must be mentioned that the heat treatment of the wet gel was in an oxygen atmosphere to decompose the hydroxyl and organics. And the gel powder was transformed into bulk glass by melting at 1750℃ for 3 h in vacuum state (10^{-4} Torr). Three series of Yb^{3+}-doped silica glasses (series A, B, and C) were prepared by this method and each series included five samples. The glass mean composition of each sample was shown in Table 1. Yb_2O_3 content amounted to 0.03 mol% in series A and 0.15 mol% in series B and C. Both series A and B were co-doped with only increasing Al_2O_3 to investigate the effect of Al^{3+} content on the reduction of Yb^{3+} to Yb^{2+} ions. Whereas series C were co-doped with fixed Al_2O_3 (4 mol%) and increasing of P_2O_5 from C1 to C5 to study the oxidation effect of P^{5+} content on the Yb^{2+}. The results of inductively coupled plasma (ICP) analysis show that Yb_2O_3, Al_2O_3 and P_2O_5 contents in silica glasses are close to theoretical values.

Table 1 Mean compositions of three series of the Yb^{3+}-doped silica glasses (mol%)

Samples		Yb_2O_3	Al_2O_3	P_2O_5	SiO_2	Al/Yb	Al/P
	A1	0.03	0		99.97	0	
	A2	0.03	0.3		99.67	10	
#A	A3	0.03	0.45		99.52	15	
	A4	0.03	1.5		98.47	50	
	A5	0.03	3		96.97	100	
	B1	0.15	0.75		99.1	5	
	B2	0.15	1.5		98.35	10	
#B	B3	0.15	3		96.85	20	
	B4	0.15	4.5		95.35	30	
	B5	0.15	6		93.85	40	
	C1	0.15	4	1	94.85	27	4
	C2	0.15	4	2	93.85	27	2
#C	C3	0.15	4	3	92.85	27	4/3
	C4	0.15	4	4	91.85	27	1
	C5	0.15	4	9	86.85	27	4/9

To study the spectroscopic properties of Yb^{2+} and Yb^{3+} ions, the bulk silica glass was cut and polished to 2-mm-thick glass chips (Ø15 mm). The absorption spectra of these chips were recorded by using a spectrophotometer (Lambda 900 UV-VIS-NIR, Perkin-Elmer) in the spectral range of 200–1100 nm. The excitation spectrum of Yb^{2+} ions by monitoring at 520 nm was detected with a spectrophotometer (FLSP 920, Edinburgh Co., UK) pumped by a Xe-lamp. The fluorescence spectra of Yb^{2+} ions were measured under excitation at 400 nm. The near-infrared fluorescence spectra of Yb^{3+} ion were detected by using the same spectrophotometer of FLSP 920 under excitation at 896 nm from Xe-lamp. X-ray photoelectron spectroscopy (XPS) measurements were taken from the sample surface using a Thermo Scientific ESCALAB 250 setup. A monochromated Al X-ray resource (1486.6 eV) was used. The operation conditions of an X-ray generator were 15 kV and 10 mA. Ar+ ion (EX05) etching for 20 seconds was performed before the measurement. The pass energy was 25 eV and the instrumental resolution was about 0.49 eV. The energy scale was calibrated by the C1s line at 285 eV. Pulsed 980-nm laser diode excitation was used to record the fluorescence lifetime of Yb^{3+} ions on the instrument FLSP 920. Fourier transform infrared (FT-IR) spectra were recorded using a spectrophotometer (Nexus FT-IR Spectrometer, Thermo Nicolet). The cooperative luminescence spectra were measured on FLSP 920 by pumping the glass with a 980 nm laser diode. All the measurements were performed at room temperature.

3. Results and discussion

3.1 Effect of Al^{3+} ions content on the Yb^{3+} to Yb^{2+} reduction in silica glasses

Absorption, excitation and fluorescence spectra of rare earth (RE) ions are usually considered as strong evidence of the presence of divalent RE ions (e.g., Eu^{2+}, Sm^{2+}, and Yb^{2+}) in crystal or glass matrices, and the absorption intensity is a qualitative estimate of the amount of these divalent rare earth ions [25, 26, 28]. In contrast to the forbidden 4f–4f transition of Yb^{3+} ions (Xe[$4f^{13}$]), the dipole-allowed $4f^{14}$–$4f^{13}5d$ transitions of Yb^{2+} (Xe[$4f^{14}$]) generally show intense absorption (excitation) band and also broad emission band at the UV and visible regions [29]. Fig. 1 shows the excitation spectrum of the presence of Yb^{2+} ions in Yb^{3+}-doped silica glasses by monitoring the emission peak of Yb^{2+} ions at 520 nm. Three broad bands at approximately 300, 325, and 400 nm are present in the excitation spectrum, corresponding to the $4f^{14}$–$4f^{13}5d$ transitions of Yb^{2+}.

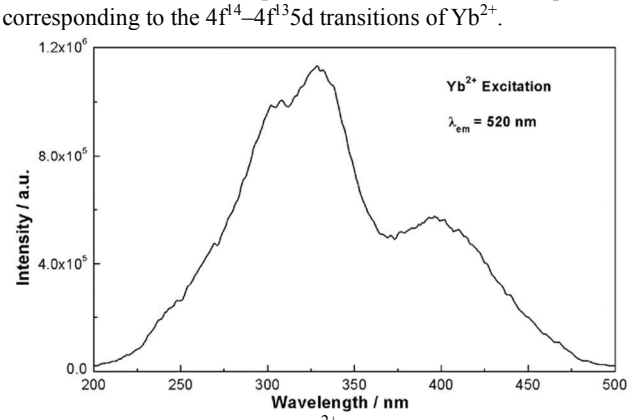

Fig. 1 Excitation spectrum of Yb^{2+} ions by monitoring emisson at

λ_{em} =520 nm in Yb^{3+}-doped silica glass (sample:B2) measured at room temperature.

Figs. 2(a) and 2(b) show the absorption and emission spectra of Yb^{2+} ions in samples of series A using Yb_2O_3 doping concentration of 0.03 mol%. The absorption of a pure silica glass prepared by sol-gel method was also shown in Fig. 2 (a) for comparison. Two conspicuous absorption bands in series A glasses are found at approximately 215 and 320–330 nm, respectively. There is also a very weak band at 300 nm in series A glasses, and the band becomes stronger in sample A5. All three bands are caused by Yb^{2+} ion absorption. The band at 320–330 nm is considered as the most conspicuous absorption peak of Yb^{2+} in Yb^{3+} and Al^{3+} co-doped silica glass [30]. As can be seen from the absorption spectrum of the pure silica glass, the two bands at 200 and 240 nm are attributed to silica host absorption. So the Yb^{2+} absorption band at 215 nm is usually superimposed on the absorption bands of silica glass host in the UV spectrum, and it also overlaps with the CT-absorption band (230 nm) of Yb^{3+} in Al^{3+} and Yb^{3+} co-doped silica glass[31–32].

As it is shown in Fig. 2 (a), with increasing of Al^{3+} content from A1 to A5, the absorption intensity at 320–330 nm gradually increases. A1 glass without no Al^{3+} ions shows the lowest absorption intensity at 320–330 nm. Sample A5 with the highest Al^{3+} content (Al/Yb = 100) in glasses possesses the strongest absorption band in 320-330 nm region.

Fig. 2 (b) shows that the emission band of the Yb^{2+} into 400 nm excitation has a maximum at approximately 520 nm. This emission band is assigned to 4f5d–4f transition of Yb^{2+} ions broaden by the existence of Yb^{2+} multisites in the glass. The emission intensity at 520 nm increases from A1 to A5, which is consistent with the variations in the absorption intensities of the samples in UV range. The increase in intensity of the absorption and emission of Yb^{2+} indicates the increase in Yb^{2+} amount with increasing Al^{3+} content from A1 to A5. It means the reduction of Yb^{3+} ions into Yb^{2+} ions is increasing in parallel with the amount of Al^{3+}ions introduced in the glass host. The reduction process of Yb^{3+} ions into Yb^{2+} is also supported by the variation in color of the Yb^{3+}-doped silica glass samples from A1 to A5. The yellow coloration appears in the silica glass A3 and intensifies from A3 to A5 is another probe of the presence of Yb^{2+} ions [33–34]. A1 and A2 are colorless because these samples contain very small amounts of Yb^{2+} ions. The inset in Fig. 2 (a) shows the yellow color of sample A4, and the surface of the glass rod is pure silica.

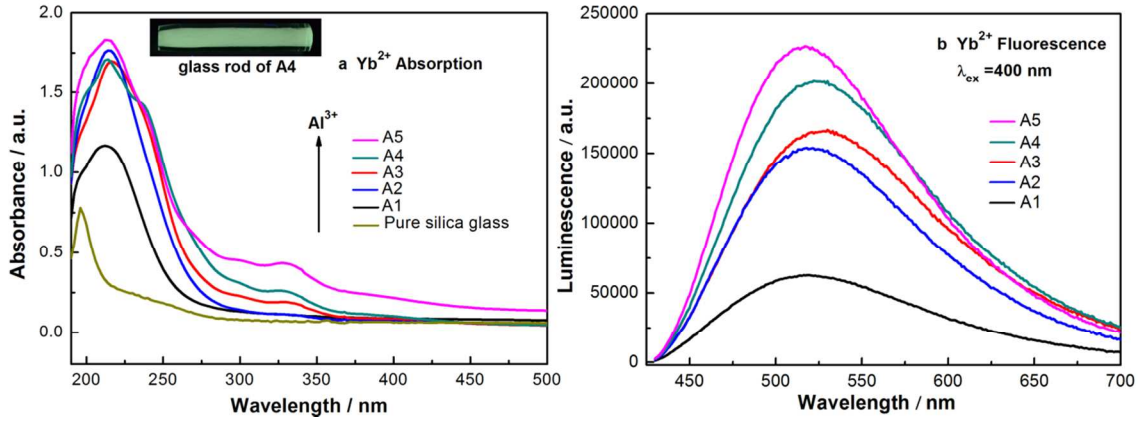

Fig. 2 Absorption (a) and fluorescence (b) spectra of Yb^{2+} ions in silica glasses of the serie A. The inset in (a) shows the yellow color of sample A4. The direction of the arrow in Fig. 2 (a) respects the increase of Al^{3+} content from A1 to A5.

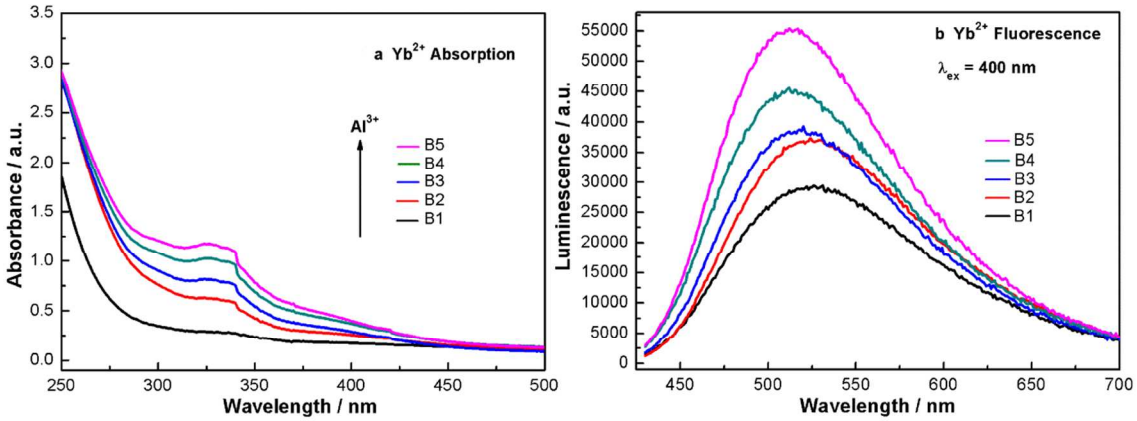

Fig. 3 Absorption (a) and fluorescence (b) spectra of Yb^{2+} ions in silica glasses of the series B. The direction of the arrow in Fig. 3 (a) respects the increase of Al^{3+} content from B1 to B5.

For further demonstration of the reducing action of Al^{3+} ions, the series B glasses with a fixed 0.15 mol% Yb_2O_3 concentration were prepared. Al_2O_3 content increases from 0.75 mol% to 6 mol% in series B, as shown in Table 1. The absorption and fluorescence

spectra of the series B glasses are shown in Fig. 3 (a) and (b). The absorption intensity at 320–330 nm increases with increasing Al_2O_3 content, which indicates that the amount of Yb^{2+} ions also increases with increasing Al_2O_3 content in the series B glasses. In Fig. 3 (b), the emission intensity of Yb^{2+} ions increases also monotonically with the increase in Al_2O_3 content, which is similar to the trend observed in Fig. 2 (b). Consequently, for Yb^{3+} singly doped and Al^{3+}/Yb^{3+}co-doped silica glass, the emission intensity of Yb^{2+} ions increases monotonically with the increasing amount of Yb^{2+} ions, which is caused by the reducing action of the gradual increasing amount of co-doped Al^{3+}.The relationship between the emission intensity of Yb^{2+} ions and Al^{3+} content is similar to that described for Sm^{2+} [35]. So the emission intensity of Yb^{2+} increases with increasing Al^{3+} ions contents.

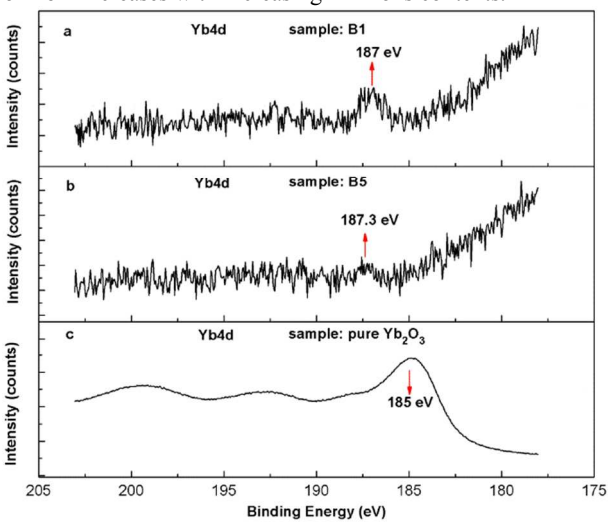

Fig. 4 XPS spectra of Yb4d in samples B1 (a), B5 (b) and the pure Yb_2O_3 powder (c)

XPS measurement is usually an effective method to detect different kinds of ions or atoms and their bonds on the material surface by analyzing the binding energy of the electron in atomic inner-shell [36]. Some researchers have measured the XPS spectra of Yb4f, 5p, 4d and 4p in $(YbS)_{1.25}CrS_2$ [37]. They revealed the multiplet structures of Yb^{2+} and Yb^{3+} ions. XPS spectra of Yb4d in samples B1, B5 and pure Yb_2O_3 (99.99%) powder were measured and listed in Fig. 4. The signal peak of Yb^{2+} ions can't be found in our samples since the Yb^{2+} content is too low to be detect at all [38]. However, the signal peak of Yb^{3+} can be detected and they are at 187 eV in sample B1 and 187.3 eV in sample B5. Comparing with pure Yb_2O_3 powder with the main peak at 185 eV, the approximate 2 eV shift in our sample is caused by the changes of the coordination environment of Yb^{3+} ions. The binding energy of Yb^{3+} ions in our samples is consistent with that in reference [39].

Under the same measure condition, the signal intensity of the Yb4d in sample B5 is weaker than that in B1. That indicates the amount of Yb^{3+} ions in B5 is less than that in B1. That is to say more Yb^{3+} ions have been reduced to Yb^{2+} ions in B5 compared with that in B1 due to more Al^{3+} ions in sample B5.

There are no Yb^{2+} ions existing in the gel power heated in an oxygen atmosphere to decompose the hydroxyl and organics. The reduction of Yb^{3+} into Yb^{2+} almost occurs during the melting process of the gel powder to form silica glass under the vacuum state. This reduction effect of Al^{3+} ions on Yb^{3+} may be related to the defect electrons (e^-) ejected from oxygen-associated hole centers (OHCs) existing in the O^{2-} matrix surrounding Yb^{3+} in the formation of the SiO_2 network [40–41]. The OHCs, chemically called O^- states [42-43], have various forms as peroxy radicals (≡Si–OO•), nonbridging-oxygen hole centers (NBOHCs, ≡Si–O•), self-trapped hole (≡Si–O•–Si≡), and aluminum-associated OHCs (Al-OHCs) [42]. These OHCs are usually thermally generated in fused silica above 500℃. The defect electron (e^-) donated by OHCs can reduce Yb^{3+} into Yb^{2+} via the following reactions:

$$O^- \rightarrow e^- + 1/2\ O_2\uparrow \quad (1)$$

$$Yb^{3+} + e^- \rightarrow Yb^{2+} \quad (2)$$

In this reduction process, the presence of Al^{3+} ions has two important effects on accelerating the reduction reaction. One is related to the increased Al-OHCs. Al^{3+} doped in silica glass behaves as the origin of the defects of Al-OHCs. In high-temperature melting state, the number of Al-OHCs increases with increasing Al^{3+} content in silica glass. One is related to the microscopic optical basicity proposed by Duffy and Ingram [43]. The addition of Al_2O_3 in silica glass can increase the optical basicity. The increased basicity can enhance the electron donation ability of the OHCs (O^-) surrounding Yb^{3+} ions [44]. Thus, the increase in Al^{3+} can increase the number of e^- and then cause the reduction of Yb^{3+} to Yb^{2+}. So the presence of Al^{3+} ions acts as an activating agent to intensify the reduction of Yb^{3+}. Moreover, the reaction (1) can also explain why Yb^{3+} can be reduced easily under the vacuum state but difficultly in an oxygen atmosphere.

3.2 Effect of P^{5+} ions content on the Yb^{2+} to Yb^{3+} oxidation in silica glasses

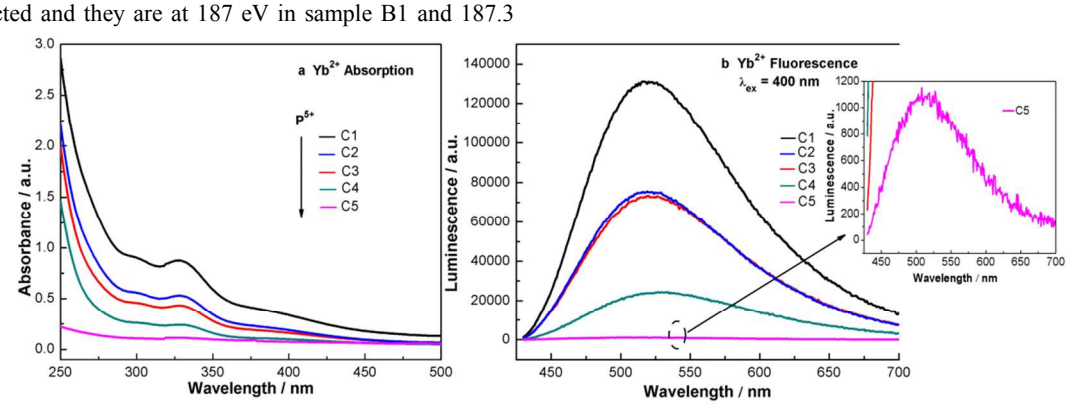

Fig. 5 Absorption (a) and fluorescence (b) spectra of Yb^{2+} ions in silica glasses of the series C. The inset in (b) is an enlargement of the

emission intensity of sample C5 between 0–1200 (a.u.).

Fig. 5 shows absorption and fluorescence spectra of Yb^{2+} ions in series C glasses. It is obviously seen that the addition of P^{5+} ions can greatly reduce the absorption and emission intensity of Yb^{2+} ion. Especially, for the sample C5, there is almost no absorption of Yb^{2+} ion at around 330 nm. The emission intensity of C5 is two orders of magnitude lower than that of C1. It indicates a great decreasing of the Yb^{2+} ions with increasing P^{5+} content.

The XPS spectra of Yb4d in samples C1 and C4 were shown in Fig. 6. We can still see the signal peak intensity in C4 is stronger than that in C1. That means more Yb^{2+} ions were oxidized into Yb^{3+} ions in sample C4 due to more content of P^{5+} ions in C4.

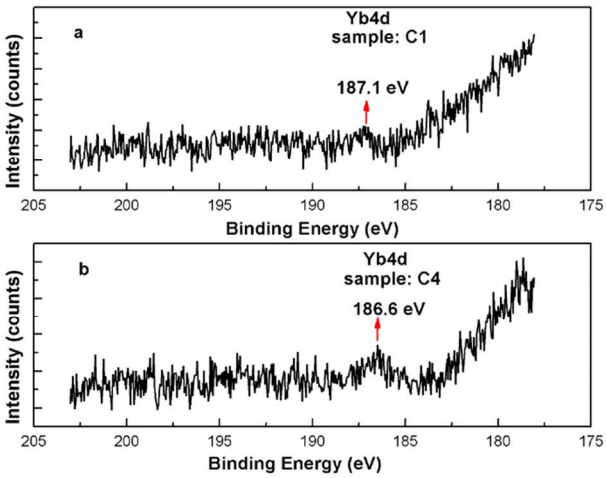

Fig. 6 XPS spectra of Yb4d in samples C1 (a) and C4 (b)

The oxidation effect of P^{5+} on Yb^{2+} may be explained by two aspects: One is related to the microscopic optical basicity. From the data provided from Duffy [45], the optical basicity of SiO_2, Al_2O_3 and P_2O_5 are 0.48, 0.6 and 0.33, respectively. When P_2O_5 was added, it will suppress the increase of the optical basicity caused by Al_2O_3 by forming $[AlPO_4]$ structure with similar optical basicity of SiO_2 [46]. Then the electron donation ability of the OHCs (O^-) is hindered. The other one is attributed to the strong tendency of P^{5+} to form a lower oxidation state (P^{4+}) to match Si^{4+} and enhance the stability of the glass. The oxidation reaction is shown as follows.

$$P^{5+} + Yb^{2+} \rightarrow P^{4+} + Yb^{3+} \quad (3)$$

It is suggested that the defect electron (e-) donated by OHCs has no chance to react with Yb^{3+} but with P^{5+} due to its strong electronegativity. The reaction is shown as follows.

$$P^{5+} + e^- \rightarrow P^{4+} \quad (4)$$

3.3 Influences of Al^{3+} and P^{5+} ions contents on the near-infrared luminescence of Yb^{3+} ions

Fig. 7 presents the representative absorption and fluorescence spectra of Yb^{3+} in sample A4, and the inset in Fig. 7 (b) shows energy level scheme of Yb^{3+} ion. It is well known that Yb^{3+} ions have only two Stark-split energy manifolds: the $^2F_{7/2}$ ground state and the $^2F_{5/2}$ excited state. Stark levels are distributed in these manifolds and labelled from 1 to 4 in the ground state and from 5 to 7 in the excited state from the lowest to the highest energy, respectively.

The broad absorption band with the peak at around 915 nm is attributed to the transition of 1→7. The strongest absorption around 975 nm relates to the transition from the lowest Stark level of the ground $^2F_{7/2}$ (1) state to the lowest Stark level of the excited state $^2F_{5/2}$ (5). The four Lorentzian curves shown in Fig. 7 (b) correspond to the transition from the excited $^2F_{5/2}$ level (5) to the $^2F_{7/2}$ ground state 1, 2, 3, and 4, respectively.

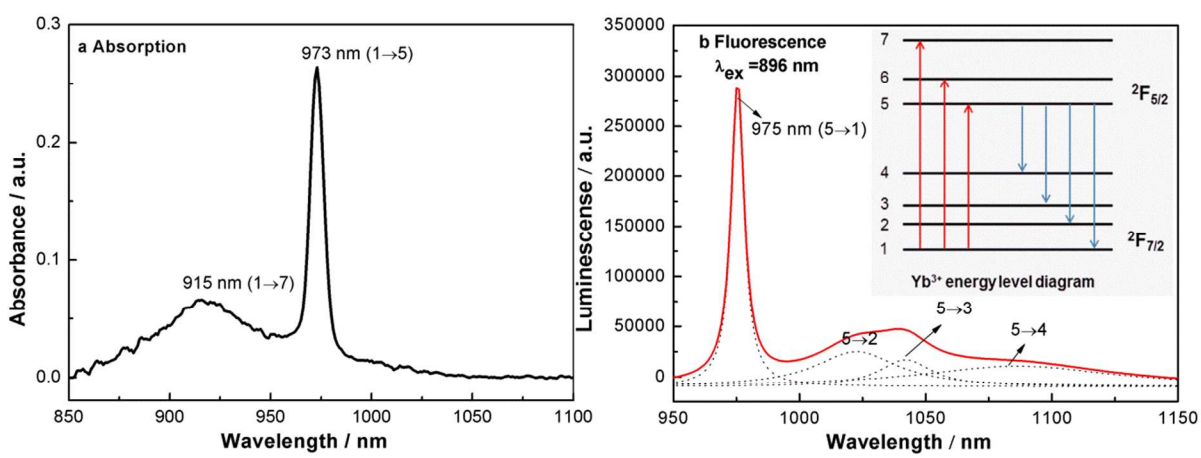

Fig. 7 (a) Absorption and (b) fluorescence spectra (black solid line) of Yb^{3+} ions in sample A4 measured at room temperature. In Fig. 7 (b), the dotted lines show Lorentzian curves, and the red line is the fitted line from the four Lorentzian curves. The inset shows the Yb^{3+} ions energy level diagram.

To study the influences of Al^{3+} and P^{5+} ion contents on the near-infrared luminescence of Yb^{3+} ions, the fluorescence spectra of Yb^{3+} ions under 896 nm excitation for the samples of series A , B, and C, respectively, are shown in Fig. 8. The Yb^{3+} $^2F_{5/2} \rightarrow {}^2F_{7/2}$ zero-phonon line (5→1 shown in the inset in Fig. 7(b)) is clearly seen in the emission spectra at 975 nm in series A and B, and 976 nm in series C. For both series A and B in which we observe only Al_2O_3 dependence in silica glasses with very similar spectroscopic properties to those of other Yb^{3+}-doped CAS and

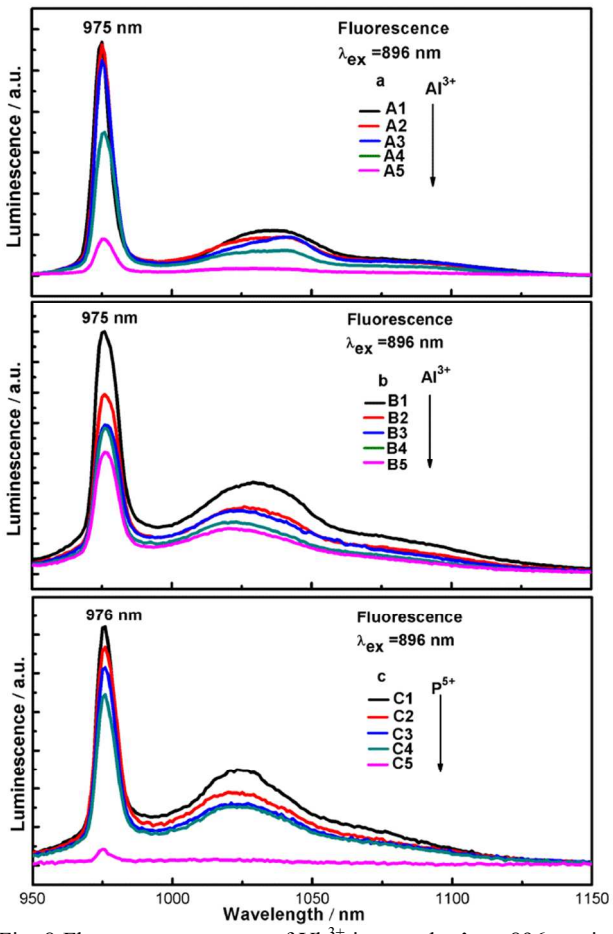

Fig. 8 Fluorescence spectra of Yb^{3+} ions under λ_{ex} =896 nm in samples of the series A (a), B (b) and C (c) respectively.

LSCAS silica glasses [47]. We observe the emission intensity of Yb^{3+} decreases with increasing Al^{3+}. Two aspects can account for this variation. On the one hand, the number of Yb^{3+} ions decreases gradually with increasing Al^{3+} because of the reduction effect of Al^{3+} ions. On the other hand, the intensity of Yb^{3+} is sensitive to the local structure surrounding Yb^{3+} ions, and the local structure is greatly affected by the Al^{3+} ions content [48]. Although a moderate quantity of Al^{3+} can decrease clustering of RE (Yb^{3+}) ions in silica glass and enhance its emission intensity [48-49], further addition of Al^{3+} ions can decrease the emission intensity [50]. There would be an optimal Al/Yb ratio at which the emission intensity of Yb^{3+} can reach the maximum value. Usually the optimal Al/Yb ratio ranges from 5 to 10 [50-51]. For series C in which we observe both Al_2O_3 and P_2O_5 dependences, the emission intensity of Yb^{3+} can be greatly reduced by the presence of P^{5+}, especially when the molar ratio of Al/P <1 as in sample C5. In Yb^{3+}-doped silica glass, when the content P^{5+}>Al^{3+}, RE ions preferentially couple with P=O radicals rather than with Al–O, probably because all aluminum ions bond to phosphorus to create [$AlPO_4$] units [46]. Raman spectra of series C shown in Fig. 9 confirms the existence of [$AlPO_4$] and P=O radicals. Compared with C1, the broader band at 1155 cm^{-1} indicates more [$AlPO_4$] units have formed in C4. The peak at 1320 cm^{-1} is due to P=O bonds [51-52]. The broad band at 1000–1250 cm^{-1} with stronger peak at 1104 cm^{-1} is ascribed to the contribution from Si-O-Si, Si-O-Al, P-O-Al, and Si-O-P bonds [52-53]. Usually concentration quenching process depends strongly on hydroxyl group concentration and rare earth impurities. In these samples the hydroxyl group concentrations should be comparable in all A, B and C samples and the rare earth impurities like Er^{3+} and Tm^{3+} ions have not been detected by up-conversion and ICP techniques. As we know, with increasing P^{5+} content, the number of Yb^{3+} ions increases. So, the decrease in emission intensity of Yb^{3+} in samples C4 and C5 may be attributed to the increase in non-radiative transition probability caused by higher average phonon energy of the [$AlPO_4$] units (1155 cm^{-1}) and P=O bond (1330 cm^{-1}) than the Si-O bond (~1100 cm^{-1}).

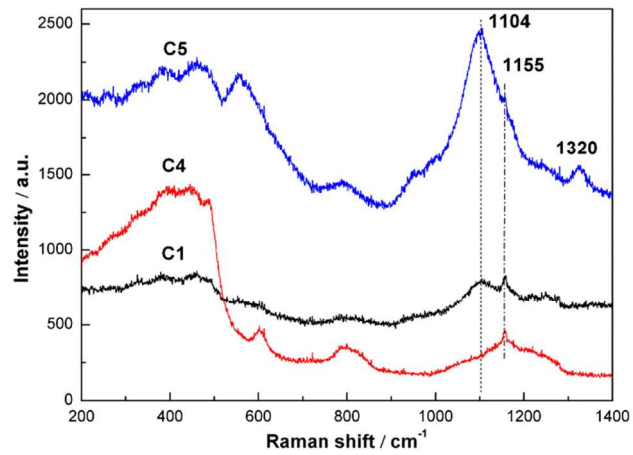

Fig. 9 Raman spectra of silica glasses of the series C

3.4 Effects of Al^{3+} and P^{5+} ions contents on the cooperative emission of Yb^{3+} ions pairs

Since the first observation by Nakazawa and Shionoya in $YbPO_4$ [54], cooperative luminescence of ytterbium ions has been reported in several hosts, crystals or glasses [55-56]. Cooperative luminescence is indeed an effective way to indicate the formation of Yb^{3+} pairs and clusters in crystals and glasses. The cooperative emission center is assigned either from two Yb^{3+} neighboring ions isolated in the host or even from Yb^{3+} aggregates. The cooperative luminescence results from the simultaneous de-excitation of two Yb^{3+} ions in the green range at around 500 nm which corresponds to the twice energy of the IR emission spectrum of the Yb^{3+} isolated ions [54]. The cooperative emission process can be expressed as follows [54]:

$$Yb^{3+}(^2F_{5/2})+Yb^{3+}(^2F_{5/2})\rightarrow Yb^{3+}(^2F_{7/2})+Yb^{3+}(^2F_{7/2})+h\nu \qquad (5)$$

The intensity of cooperative emission depends on the shortest distance d between Yb^{3+} ions [57]. This cooperative fluorescence emission has a very low efficiency and naturally is favored for the shortest distances between Yb^{3+} ions. The calculation of the shortest distance d between Yb^{3+} ions in the dipole-dipole interaction has been estimated at d=4.5Å [57]. The cooperative emission probability is proportional to d^{-8}. In Sc_2O_3 sesquioxide, cooperative luminescence has been used to demonstrate an homogeneous distribution of Yb^{3+} in the host [58]. Cooperative luminescence has also already been used as structural probe in glasses to optimize the composition and to prevent clustering or to analyze the influence of the glass composition in Yb^{3+}-doped aluminosilicate, borosilicate and phosphate glasses [57, 59]. A

good correlation has been found in the phosphate glasses between the structural evolution of the glass and the cooperative emission intensity.

To study the dispersion effects of Al^{3+} and P^{5+} on Yb^{3+}, the spectra of the cooperative emission of series B and C glasses at approximately 500 nm were obtained by pumping the glass with a 980 nm laser diode and are shown in Fig 10. The inset in Fig. 10 (a) is the picture of green light of cooperative luminescence of Yb^{3+} ions observed in sample B2. The influence of impurities of Tm^{3+} and Er^{3+} on up-conversion emission is negligible because no Tm^{3+} and Er^{3+} were detected in series B and C glass by ICP.

The reduction of the cooperative emission intensity with increasing Al^{3+} and P^{5+} contents is evident, although changes in the intensities among C2, C3 and C4 are minimal. We observe effectively a progressive reduction of Yb^{3+} pairs with increasing Al_2O_3 or P_2O_5 concentration. Thus, even with a very high concentration of SiO_2 in all A, B and C series, a few percentage of Al^{3+} and P^{5+} ions in silica glasses (table 1) shows a good dispersion effect on Yb^{3+} ions. From the aspect of the relation between the structural evolution of the glass and the cooperative emission intensity [59], the silica glasses of series A, B and C have the evolution tendency of the dimensionality from three-dimensional (3D) to 2D network with increasing Al_2O_3 or P_2O_5 concentration. Series C samples are special ones with the double effect of Al_2O_3 and P_2O_5 contents to disperse Yb^{3+} ions. Particularly, we are able to detect almost no more pairs or clusters in sample C5 when the content $P^{5+} > Al^{3+}$ with the molar ratio Al/P=4/9 (Figure 10 b). As we have discussed above that Yb^{3+} ions preferentially couple with P=O radicals rather than with Al–O when the content $P^{5+} > Al^{3+}$ in Yb^{3+}-doped silica glass. The cooperative luminescence result of C5 indicates that P^{5+} ions have a better dispersion effect on Yb^{3+} ions than Al^{3+} ions in Yb^{3+}-doped silica glass.

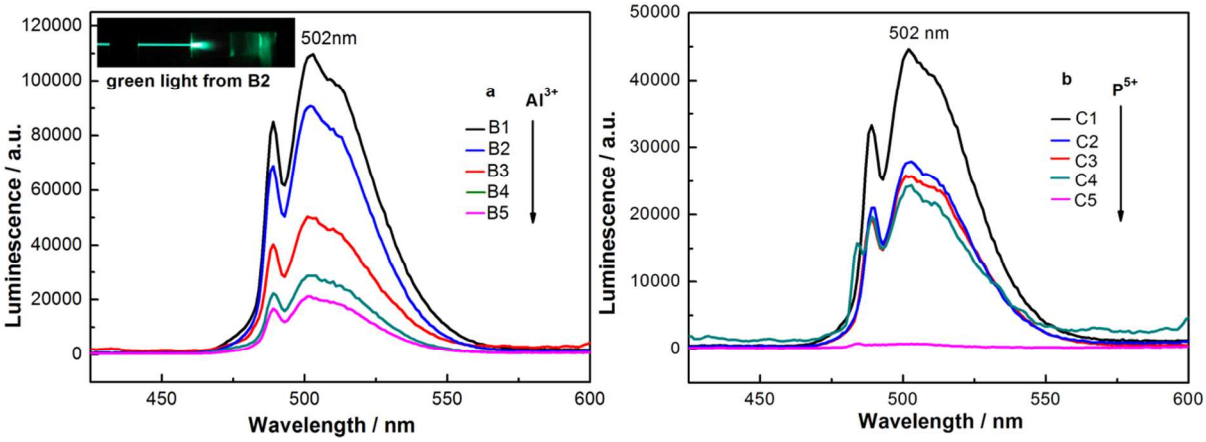

Fig. 10 Cooperative luminescence spectra of samples of series B (Al_2O_3 content dependence) (a) and C (Al_2O_3 and P_2O_5 contents dependence) (b) upon excitation at 980 nm by laser diode. The inset in (a) shows the picture of green cooperative luminescence of Yb^{3+} ions in sample B2.

4. Conclusion

Sol-gel method is a good way to produce a large-size Yb^{3+}-doped silica glass with broad composition region and good doping homogeneity. By using this method, three series of Yb^{3+}-doped silica glasses containing different amounts of Al_2O_3 and P_2O_5 were prepared. For the first time, the influences of Al^{3+} and P^{5+} ions contents on the valence state of ytterbium ions were studied systematically. The influences of Al^{3+} and P^{5+} ions contents on the near-infrared luminescence of Yb^{3+} ions and cooperative luminescence intensity of Yb^{3+} ions pairs were also studied in detail. The results are helpful to solve some important problems in Yb^{3+}-doped silica fiber laser such as high background optical loss and photodarkening which were partly due to the existence of Yb^{2+} ions and Yb^{3+} ions pairs in Yb^{3+}-doped silica glass.

With increasing Al^{3+} or P^{5+} ions content in Yb^{3+}-doped silica glass, the Yb^{3+} to Yb^{2+} reduction or the Yb^{2+} to Yb^{3+} oxidation was greatly accelerated. The reduction mechanism of Al^{3+} ions on Yb^{3+} ions is explained by the microscopic optical basicity of silica glass and the ejection of one defect electrons (e-) from oxygen-associated hole centers. With increasing Al^{3+} ions, both the microscopic optical basicity of silica glasses and the number of Al-OHCs will increase. And especially, the increased optical basicity can enhance the electron donation ability of the OHCs surrounding Yb^{3+} ions. Thus, Al^{3+} will increase the number of e- and then promote the reduction of Yb^{3+} to Yb^{2+} ions. But with increasing P^{5+} ions, the microscopic optical basicity of silica glass will be lowered down. At the same time, to match Si^{4+} and enhance the stability of silica glass, P^{5+} ions have a strong tendency to form a lower oxidation state (P^{4+}). Thus, the oxidation of Yb^{2+} to Yb^{3+} ions will be promoted by P^{5+} ions.

The near-infrared luminescence intensity of Yb^{3+} ions decrease gradually with increasing Al^{3+} and P^{5+} ions contents. So, the addition of Al^{3+} and P^{5+} ions content in Yb^{3+}-doped silica glass to solve the clustering of Yb^{3+} ions should be moderate. A clear dispersion effect of Yb^{3+} ions in silica glasses has been observed by the introduction of Al^{3+} and P^{5+} ions, detected with the help of the cooperative luminescence spectra. Moreover, from the cooperative luminescence intensity comparison between sample C5 and C1–C4, we can see that P^{5+} ions have a better dispersion effect on Yb^{3+} ions than Al^{3+} ions in Yb^{3+}-doped silica glass.

Acknowledgments

This research was financially supported by the Chinese National Natural Science Foundation (No. 60937003). The authors would like to thank Mr. Yirong Mao for his assistance during the glass sintering experiments.

Notes and references

[a] *Shanghai Institute of Optics and Fine Mechanics, Chinese Academy of Sciences,* No. 390, Qinghe Road, Jiading District, Shanghai 201800, China. E-mail: woshiwsk@163.com; Fax: +86-21-5991-4516; Tel: +86-21-5991-4297.* E-mail of corresponding author:woshiwsk@163.com.
[b] *Graduate School of Chinese Academy of Sciences, Beijing 100039, China.*
[c] *Faculty of Chemistry, University of Wrocław, 14, F. Joliot-Curie, PL-50-383, Wrocław, Poland.*
[d] *Institute Light Matter (ILM), UMR 5306 University of Lyon 1-CNRS, University of Lyon, 69622, Villeurbanne, France.*

1 M. M. Bubnov, V. N. Vechkanov, A. N. Gur'yanov, K. V. Zotov, D. S.Lipatov, M. E. Likhachev and M. V. Yashkov, *Inorg. Mater.*, 2009, **45**, 444–449.
2 W. Li, Q. Zhou, L. Zhang, S. Wang, M. Wang, C. Yu, D. Chen, L. Hu, Chin, *Opt. Lett.*, 2013, **11**, 091601-(1-3).
3 T. Wei, J. Li, J. Zhu, Chin, *Opt. Lett.*, 2012, **10**, 040605-(1-4).
4 G. Almantas, *Opt. Photon. News*. 2004, **15**, 42–47.
5 R. Zhu, J. Wang, J. Zhou, J. Liu, W. Chen, Chin, *Opt. Lett.*, 2012, **10**, 091402-(1-4).
6 C. Zhou, Y. Liu, R. Zhu, S. Du, X. Hou, W. Chen, Chin, *Opt. Lett.,* 2013, **11**, 081403-(1-3)
7 S. H. Glenzer, B. J. MacGowan, P. Michel, N. B. Meezan, L. J. Suter, S. N. Dixit, J. L. Kline, G. A. Kyrala, D. K. Bradley, D. A. Callahan, E. L. Dewald, L. Divol, E. Dzenitis, M. J. Edwards, A. V. Hamza, C. A. Haynam, D. E. Hinkel, D. H. Kalantar, J. D. Kilkenny, O. L. Landen, J. D. Lindl, S. LePape, J. D. Moody, A. Nikroo, T. Parham, M. B. Schneider, R. P. Town, P. Wegner, K. Widmann, P. Whitman, B. K. Young, B. Van Wonterghem, L. J. Atherton and E. I. Moses, *Science*, 2010, **327**, 1228–1231.
8 J. K. Sahu, S. Yoo, A. J. Boyland, A. Webb, C. Codemard, R. J. Standish and J. Nilsson, OSA / CLEO/QELS, 2010.
9 T. A. Birks, J. C. Knight and P. St. J. Russell, *Opt. Lett.*, 1997, **22**, 961–963.
10 K. Arai, H. Namikawa, K. Kumata, T. Honda, Y. Ishii, T. Hada, J. *Appl. Phys.*, 1986, **59**, 3430–3436.
11 J. Laegsgaard, *Phys. Rev. B*, 2002, **65**, 174114 -(1–10).
12 S. Sen, R. Rakhmatullin, R. Gubaydullin, A. Poppl, *Phys. Rev. B,* 2006, **74**, 100201–(1–4).
13 C. Wang, G. Zhou, Y. Han, W. Wang, C. Xia, L. Hou, Chin, *Opt. Lett.*, 2013, **11**, 061601-(1-4).
14 M. Engholm and L. Norin, *Opt. Express*, 2008, **16**, 1260-1268.
15 M. E. Likhachev, S. S. Aleshkina, A. V. Shubin, M. M. Bubnov, E. M. Dianov, D. S. Lipatov, A. N. Guryanov, in: European Conference on Lasers and Electro-Optics, Munich, Germany, 2011, May 22–26.
16 J. Koponen, M. Söderlund, H. J. Hoffman, D. Kliner, and J. Koplow, *Proc. of SPIE*, 2006, **6453**, 64531E–(1–10).
17 T. Kitabayashi, M. Ikeda, M. Nakai, T. Sakai, K. Himeno, and K. Ohashi, in:Optical Fiber Communication Conference, Anaheim, California, 2006, March 5.
18 S. Unger, A. Schwuchow, S. Jetschke, V. Reichel, A. Scheffel, J. Kirchhof, *Proc. of SPIE*, 2008, **6890**, 689016–(1–11).
19 Y. Shen, Q. Sheng, S. Liu, W. Li and D. Chen. Chin. *Opt, Lett.,* 2013, **11**, 051601–(1–3).
20 S. Unger, A. Schwuchow, S. Jetschke, V. Reichel, A. Scheffel, J. Kirchhof. *Proc. of SPIE*, 2008, **6890**, 689016–(1–11).
21 I. Nicoara, N. Pecingina-Garjoaba and O. Bunoiu, *J. Cryst. Growth*, 2008, **310**, 1476–1481.
22 J. Kirchhof, S. Unger, A. Schwuchow, S. Grimm, V. Reichel, *J. Non-Cryst. Solids,* 2006, **352**, 2399–2403.
23 J. Kirchhof, S. Unger, A. Schwuchow, S. Jetschke, V. Reichel, M. Leich, A. Scheffel, *Proc. of SPIE*, 2010, **7598**, 75980B–(1–11).
24 S. Rydberg and M. Engholm. Opt. Express, 2013, 21, 6681-6688.
25 A. Biswas, C. S. Friend, P. N. Prasad, *Mater. Lett.,* 1999, **39**, 227–231.
26 M. Nogami, N. Hayakawa, N. Sugioka, Y. Abe, *J. Am. Ceram. Soc*, 1996, **79**,1257–61.
27 S. Wang, Z. Li, C. Yu, M. Wang, S. Feng, Q. Zhou, D. Chen, L.Hu, *Opt. Mater.,* 2013, **35**, 1752–1755.
28 P. Yang, P. Deng, Z. Yin, *Journal of Lumin.,* 2002, **97**, 51–54.
29 Y. Huang, P. Wei, S. Zhang and H. J. Seo, *J. Electrochem. Soc.*, 2011, **158**, H465–H470.
30 J. Kirchhof, S. Unger, A. Schwuchow, S. Jetschke, V. Reichel, M. Leich, A. Scheffel, *Proc. of SPIE*, 2010, **7598**, 75980B–(1–11).
31 M. Engholm and L. Norin, *Opt. Express,* 2008, **16**, 1260–1268.
32 M. Engholm, L. Norin and D. Aberg, *Opt. Express*, 2007, **32**, 3352–3354.
33 J. Kirchhof, S. Unger, A. Schwuchow, S. Grimm and V. Reichel, *J. Non-Cryst. Solids*, 2006, **352**, 2399–2403.
34 J. Broeng, A. Langner, G. Schötz, M. Such, T. Kayser, V. Reichel, S. Grimm, J. Kirchhof, V. Krause, G. Rehmann, *Proc. of SPIE*, 2008, **6873**, 687311(1–9).
35 M. Nogami and Y. Abe, J. Appl. Phys., 1997, **81**, 6351–6356.
36 Y. Sorek, M. Zevin, and R. Reisfeld, Chem. Mater. 1997, **9**, 670–676.
37 Y.Ohno, J. Electron. Spectrosc. Relat. Phenom., 2008, **165**, 1–4.
38 O. M. ten Kate, H. T. Hintzen, P. Dorenbos and E. van der Kolk, J. Mater. Chem., 2011, **21**, 18289–18294.
39 P. Ramasamy, P. Chandra, S. W. Rhee and J. Kim, Nanoscale, 2013, **5**, 8711–8717.
40 M. A. Zaitoun, T. Kim and C. T. Lin, *J. Phys. Chem. B*, 1998, **102**, 1122–1125.
41 A. Biswas, C. S. Friend, P. N. Prasad, *Mater. Lett.*, 1999, **39**, 227–231.
42 F. Freund and M. M. Masuda, J. Mater. Res., 1991, 6, 1619–1622.
43 J. A. Duffy and M. D. Ingram, *J. Non-Cryst. Solids*, 1976, **21**, 373–410.
44 J. A. Duffy, *J. Non-Cryst. Solids*, 2002, **297**, 275–284.
45 J. A. Duffy, M. D. Ingrain, C．R． Chimie, 2002, 797-804.
46 G. G. Vienne, W. S. Brockesby, R. S. Brown, Z. J. Chen, J. D. Minelly, J. E. Roman and D. N. Payne, *Opt. Fiber. Thchnol.*, 1996, **2**, 387–393.
47 Y. Guyot, A. Steimacher, M. P. Belançon, A. N. Medina, M. L. Baesso, S. M. Lima, L. H. C. Andrade, A. Brenier, A. M. Jurdyc and G. Boulon, *J. Opt. Soc. Am. B.*, 2011, **28**, 2510–2517.
48 M. Nogami and Y. Abe, J. Appl. Phys., 1997, 81, 6351–6356.
49 Y. Qiao, L. Wen, B. Wu, J. Ren, D. Chen and J. Qiu, *Mater. Chem. Phys.*, 2008, **107**, 488-491.
50 S. Liu, H. Li, Y. Tang, L. Hu, Chin, *Opt. Lett.*, 2012, **10**, 081601–081604.
51 K. Arai, H. Namikawa, K. Kumata, T. Honda, Y. Ishii and T. Handa. *J. Appl. Phys.*, 1986, **59**, 3430–3436.
52 S. G. Kosinski, D. M. Krol, T. M. Duncan, D. C. Douglass, J. B. Macchesney and J. R. Simpson, *J. Non-Cryst. Solids*, 1988, **105**, 45–52.
53 J. Ding, Y. Chen, W. Chen, L. Hu, G. Boulon, Chin, *Opt. Lett.*, 2012, **10**, 071602-(1-4).
54 E.Nakazawa and S. Shionoya, Phys. Rev. Lett., 1970, 25, 1710–1712.
55 P. Goldner, F. Pellé, D. Meichenin and F. Auzel, *J. Lumin.*, 1997, **71**, 137–150.
56 G. Boulon, Co-operative processes in Yb^{3+}-doped materials. Frontiers Developments in Optics and Spectroscopy, B. Di Bartolo and O. Forte. Book available free on http://www.bc.edu/schools, September 2007, p.5-1, 5-22.
57 T. Deschamps, N. Ollier, H. Vezin, and C. Gonnet, *J. Chem. Phys.*, 2012, **136**, 014503-(1–4).
58 V. Lupei, A. Lupei, G. Boulon, A. Jouini, A. Ikesue, *J. Alloys Compd.*, 2008, **451**, 179-181.
59 B. Schaudel, P. Goldner, M. Prassas, F. Auzel, *J. Alloys Compd.,* 2000, **300-301**, 443-449.

